

Published in final edited form as:

J Biol Chem. 2006 December 22; 281(51): 39693–39698. doi:10.1074/jbc.M609384200.

A Molecular Mechanism for the Heparan Sulfate Dependence of Slit-Robo Signaling*

Sadaf-Ahmahni Hussain[‡], Michael Piper^{§,1}, Noémi Fukuhara^{‡,2}, Laure Strohlic[§], Gian Cho[‡], Jason A. Howitt^{‡,3}, Yassir Ahmed[¶], Andrew K. Powell[¶], Jeremy E. Turnbull^{¶,4}, Christine E. Holt[§], and Erhard Hohenester^{‡,5}

[‡]Division of Cell and Molecular Biology, Imperial College London, London SW7 2AZ

[§]Department of Physiology, Development and Neuroscience, University of Cambridge, Downing Street, Cambridge CB2 3DY

[¶]Molecular Glycobiology Group, School of Biological Sciences, University of Liverpool, Crown Street, Liverpool L69 7ZB, United Kingdom

Abstract

Slit is a large secreted protein that provides important guidance cues in the developing nervous system and in other organs. Signaling by Slit requires two receptors, Robo transmembrane proteins and heparan sulfate (HS) proteoglycans. How HS controls Slit-Robo signaling is unclear. Here we show that the second leucine-rich repeat domain (D2) of Slit, which mediates binding to Robo receptors, also contains a functionally important binding site for heparin, a highly sulfated variant of HS. Heparin markedly enhances the affinity of the Slit-Robo interaction in a solid-phase binding assay. Analytical gel filtration chromatography demonstrates that Slit D2 associates with a soluble Robo fragment and a heparin-derived oligosaccharide to form a ternary complex. Retinal growth cone collapse triggered by Slit D2 requires cell surface HS or exogenously added heparin. Mutation of conserved basic residues in the C-terminal cap region of Slit D2 reduces heparin binding and abolishes biological activity. We conclude that heparin/HS is an integral component of the minimal Slit-Robo signaling complex and serves to stabilize the relatively weak Slit-Robo interaction.

Slits are large secreted leucine-rich repeat (LRR)⁶ proteins with multiple roles in cell signaling and adhesion. They have well established and evolutionarily conserved functions as guidance cues in the developing nervous system (1, 2), but Slits are also important in the development of the vasculature (3) and other organs (4). The first class of Slit receptors to be identified were Robo family members, which are transmembrane proteins with an

*This work was supported by grants from the Wellcome Trust (to E. H. and C. E. H.) and the Biotechnology and Biological Sciences Research Council (to A. K. P. and J. E. T.).

© 2006 by The American Society for Biochemistry and Molecular Biology, Inc.

⁵Wellcome senior research fellow. To whom correspondence should be addressed: Division of Cell and Molecular Biology, Biophysics Section, Blackett Laboratory, Imperial College London, London SW7 2AZ, UK. Tel.: 44-20-7594-7701; Fax: 44-20-7589-0191; e.hohenester@imperial.ac.uk.

¹Present address: The Queensland Brain Institute, St. Lucia, Queensland 4072, Australia.

²EMBO postdoctoral fellow.

³Present address: Howard Florey Institute, University of Melbourne, Parkville, Victoria 3010, Australia.

⁴Medical Research Council senior research fellow.

The costs of publication of this article were defrayed in part by the payment of page charges. This article must therefore be hereby marked "advertisement" in accordance with 18 U.S.C. Section 1734 solely to indicate this fact.

⁶The abbreviations used are: LRR, leucine-rich repeat; HS, heparan sulfate; hSlit2, human Slit2; CT, C-terminal; FGF, fibroblast growth factor; FGFR, FGF receptor; TBS, Tris-buffered saline.

extracellular domain resembling cell adhesion molecules and a large cytosolic signaling domain (1, 2). Biochemical studies have defined the domains mediating the Slit-Robo interaction (5, 6), as well as some of the components of the signaling cascade downstream of Robo activation (7, 8), but how binding of Slit to Robo receptors conveys a signal across the cell membrane remains unknown.

The first indication that there might exist a second Slit receptor came from the observation that heparan sulfate (HS) was required for the repellent activity of Slit *in vitro* (9) and *in vivo* (10). The identity of this receptor was revealed by recent genetic studies in invertebrates, which showed that Slit signaling requires Robo to be co-expressed on the same cell with the HS proteoglycan syndecan (11–13). Syndecan is a membrane-spanning protein to which are covalently attached several HS chains, consisting of repeating sulfated disaccharide units (14). Heparin is a member of the HS family that is more highly and uniformly sulfated than other HS. Johnson *et al.* (12) showed that both Slit and Robo can be co-immunoprecipitated with syndecan, suggesting the presence of a ternary (or higher order) complex at the neuronal cell membrane. However, the composition and functional relevance of this putative ternary complex was not established. Because the Slit distribution was found to be altered in syndecan-deficient embryos, HS may also be required for Slit localization rather than signaling (12).

Here we provide direct biochemical and functional evidence for a ternary signaling complex composed of the second LRR domain of Slit, Robo, and heparin/HS. Other Slit domains are dispensable for signaling in an *in vitro* growth cone collapse assay, but heparin/HS is required absolutely. We conclude that heparin/HS is an integral component of the minimal Slit-Robo signaling complex.

EXPERIMENTAL PROCEDURES

Expression Vectors

All constructs were made by PCR amplification from complete cDNA clones, kindly provided by Dr. Guy Tear (King's College, London, UK) and Dr. Lindsay Hinck (University of California, Santa Cruz). Primer sequences are available upon request. The PCR products were cloned into modified pCEP-Pu vectors, coding for proteins with a His tag either at the N terminus (Slit constructs) or at the C terminus (Robo constructs). A Robo IG1–5 Fc construct was made by replacing the C-terminal His tag with a human Fc sequence obtained by PCR amplification from the pFUSE-hFc1 vector (InvivoGen). Mutations in human Slit2 (hSlit2) D2 were introduced by strand overlap extension PCR. The insert sequences of all expression vectors were verified by DNA sequencing. The domain boundaries of the Slit LRR domains and the Robo D1–5 construct have been described previously (5). The new constructs have the following boundaries (sequence numbering includes the signal peptide): Slit EG1–5, NACFE ... YPQTS (933–1137); Slit EG6-LG-EG7, QTSPC ... TVTAA (1134–1430); Slit CT, QGEGS ... TKKCY (1417–1504); Slit EG6-LG-EG7-CT, QTSPC ... TKKCY (1134–1504); hSlit2 D2, SVLHC ... FADLA (269–505); Robo D1–2, GQYQS ... IVQVK (51–254); Robo D3–5, KPYFM ... AADPS (254–546). The following vector-derived sequences are additionally present in the mature proteins: APLVHHHHHHALA and APLA, respectively, at the N terminus of all Slit and Robo constructs; AAAHHHHHHH at the C terminus of His-tagged Robo constructs; and AAAVECPP ... SLSPG at the C terminus of the Robo IG1–5 Fc construct.

Protein Production

All proteins were purified from the conditioned medium of episomally transfected 293-EBNA cells as described (5). Briefly, cells were maintained in Dulbecco's modified Eagle's

medium, 10% fetal calf serum (Invitrogen), transfected using FuGENE reagent (Roche Applied Science), and selected with 1 $\mu\text{g}/\text{ml}$ puromycin (Sigma). His-tagged proteins were purified from serum-free conditioned medium using TALON affinity beads (BD Biosciences) or 5-ml HisTrap columns (GE Healthcare). The EG6-LG-EG7-CT construct was additionally purified by preparative heparin affinity chromatography. The Robo IG1–5 Fc protein was purified using protein A-Sepharose resin (Sigma). Purified proteins were dialyzed into TBS, analyzed by SDS-PAGE, and quantified by measuring their absorption at 280 nm.

Oligosaccharide Production

Defined heparin-derived oligosaccharides were prepared as described (15, 16). Briefly, bovine lung heparin (Calbiochem) was partially digested using heparinase I (IBEX Technologies, Inc.). Partial digests were fractionated by gel filtration chromatography on a Superdex 30 preparation grade column (3×200 cm) run at 0.5 ml/min in 0.5 M ammonium hydrogen carbonate. Size-defined fractions were further separated by strong anion exchange chromatography using a Propac PA1 column (0.9×25 cm; Dionex), eluting with a linear NaCl gradient (0–1 M). Pooled peak fractions were desalted and lyophilized. Purified oligosaccharides were analyzed by PAGE and quantified by weighing or by measuring their absorption at 232 nm.

Solid-phase Protein Binding Assay

The solid-phase binding assay was carried out as described (5). Briefly, Slit D1-4 (100 $\mu\text{g}/\text{ml}$) was coated onto 96-well microtiter plates (NUNC Maxisorp). Wells were blocked with TBS/casein/Tween 20 and washed with TBS. Robo IG1–5 Fc protein was added for 1 h. After four washes, bound protein was detected by alkaline phosphatase-conjugated goat anti-human Fc antibody (Sigma). In some experiments, heparin (Sigma, 10 $\mu\text{g}/\text{ml}$) was added together with Robo IG1–5 Fc.

Chromatography

All chromatography experiments were done on an Äkta system (GE Healthcare). A 5-ml heparin HiTrap column equilibrated in 50 mM Tris-HCl, pH 7.5, was used to determine heparin affinities; bound proteins were eluted with a linear NaCl gradient (0–2 M for the EG6-LG-EG7-CT construct and 0–1 M for all other constructs). Gel filtration chromatography was carried out using a 24-ml Superdex 75 column run at 0.5 ml/min in 20 mM Na-HEPES, pH 7.5, 150 mM NaCl.

Growth Cone Collapse Assay

The retinal growth cone collapse assay was performed as described (8). Briefly, *Xenopus* eye primordia were dissected from stage 35/36 embryos and cultured at 20 °C on coverslips coated with 10 $\mu\text{g}/\text{ml}$ poly-L-lysine (Sigma) and 10 $\mu\text{g}/\text{ml}$ laminin (Sigma) for 24 h. hSlit2 D2 proteins (40 nM), hSlit2 conditioned medium (positive control), or TBS (negative control) were added directly to cultured explants for 10 min. Cultures were then fixed for 1 h in 2% paraformaldehyde + 7.5% sucrose and then mounted. The number of collapsed growth cones was counted in blind conditions. Heparin or HS (Sigma; 100 $\mu\text{g}/\text{ml}$) was added immediately prior to the addition of hSlit2 D2. For cultures treated with heparinase 1 (Sigma; 2.5 units/ml), the enzyme was added 3 h before the addition of hSlit2 D2. Each experiment was conducted independently a minimum of four times.

RESULTS

Mapping of Heparin-binding Sites in Slit and Robo

To locate the heparin-binding site(s) within the large *Drosophila* Slit protein, we used a panel of recombinant proteins spanning the entire molecule. In a previous study we had shown that the LRR region of Slit consists of four distinct domains, D1–4, each comprising an array of LRRs flanked by cysteine-rich caps, and we mapped the Robo-binding site to a highly conserved region on the concave face of Slit D2 (5). In addition to the LRR domain constructs available from that study, we prepared several new constructs spanning the C-terminal portion of Slit (Fig. 1). The EG1-5 construct contains the five epidermal growth factor-like domains following the LRR region and terminates at a natural proteolytic cleavage site of Slit (1). The EG6-LG-EG7-CT construct contains the remainder of the Slit C-terminal region; a truncated version of this construct, EG6-LG-EG7, was used to assess the contribution to heparin binding of the C-terminal (CT) cystine knot domain. It was not possible to study heparin binding by the CT domain directly, as the isolated CT domain was not secreted by 293 cells transfected with the relevant expression vector.

The recombinant Slit proteins were analyzed by heparin affinity chromatography. Several proteins did not bind to the heparin column; those that did eluted in single sharp peaks, and the NaCl concentration required for elution was taken as a measure of relative heparin affinity. We found that heparin-binding sites are located at either end of the Slit protein, whereas the central portion does not interact with heparin (Fig. 1A). These findings are in agreement with an earlier study on the two natural cleavage products of hSlit2 (17). The CT domain of *Drosophila* Slit has the highest apparent affinity for heparin (compare EG6-LG-EG7-CT and EG6-LG-EG7), but the N-terminal LRR domains of Slit, D1 and D2, also bind to heparin, and their combined presence in D1–4 results in a substantial affinity for heparin.

We also tested whether the Slit-binding ectodomain of *Drosophila* Robo displays affinity for heparin. Robo IG1–5 bound quite strongly to the heparin affinity column; further dissection of this region into IG1–2 and IG3–5 showed that the heparin binding activity is fully contained within IG1–2 (Fig. 1A).

Formation of a Ternary Slit-Robo-Heparin Complex

The experiments described above demonstrate that both the Robo-binding domain of Slit (D2) (5) and the Slit-binding region of Robo (IG1–2) (6) bind heparin, raising the intriguing possibility of a ternary Slit-Robo-heparin complex. To see whether heparin had an effect on the Slit-Robo interaction, we first carried out a solid-phase binding experiment (Fig. 2) in the absence and presence of soluble heparin. Addition of 10 $\mu\text{g/ml}$ heparin resulted in a marked (greater than 10-fold) increase of the apparent affinity of Robo D1–5 Fc for Slit D1–4. Thus, heparin enhances the Slit-Robo interaction, most likely via the formation of a ternary Slit-Robo-heparin complex.

To obtain direct evidence for ternary complex formation, we used analytical gel filtration chromatography (Fig. 3A). *Drosophila* Slit D2 (27.4 kDa + two *N*-linked glycans) behaved as a monomer, as reported previously (5). The elution volume of *Drosophila* Robo IG1–2 (24.1 kDa) is also most compatible with a monomer, considering that this construct is likely to adopt an extended conformation and will therefore elute earlier than a globular protein of the same mass. When Slit D2 and Robo IG1–2 were mixed in a 1:1 ratio, a single peak was observed that eluted ahead of the individual proteins, demonstrating formation of a binary complex. SDS-PAGE showed that the peak fractions contained Slit D2 and Robo IG1–2 in comparable amounts (Fig. 3B). The Slit D2-Robo IG1–2 complex must have 1:1 stoichiometry, given that its elution volume of 10.9 ml corresponds to an ~55-kDa globular protein. The close correspondence to the calculated mass (51.5 kDa + two *N*-linked glycans)

indicates a compact shape of the complex. The shoulder at a higher elution volume may result from partial dissociation of the complex on the column.

We next tested whether addition of heparin to the minimal Slit-Robo complex results in the formation of a ternary complex. Because native heparin is too large and polydisperse to be used in these experiments, we used a purified heparin-derived decasaccharide composed of repeating trisulfated disaccharide units, which was expected to be long enough to span the minimal Slit-Robo complex. When Slit D2, Robo IG1–2, and the heparin decasaccharide were mixed in a 1:1:1 ratio, the resulting complex eluted even earlier than the binary Slit-Robo complex, indicating formation of a ternary Slit-Robo-heparin complex (Fig. 3A). SDS-PAGE of the peak fractions again demonstrated the presence of Slit and Robo in comparable amounts (Fig. 3B). Given that a heparin decasaccharide has a similar hydrodynamic radius as an ~20-kDa globular protein (18) and that the elution volume of the ternary complex corresponds to an ~70-kDa globular entity, the most likely stoichiometry of the ternary Slit-Robo-heparin complex is 1:1:1. Interestingly, when the heparin decasaccharide was added to the individual Slit D2 and Robo IG1–2 proteins, no interaction was detected by gel filtration chromatography (data not shown), suggesting that a high affinity binding site is only formed in the Slit-Robo complex.

Heparin-dependent Biological Activity of Slit D2

Our biochemical observation of a minimal Slit-Robo-heparin complex suggests that an important function of heparin/HS in Slit-Robo signaling may be to strengthen the association of Slit domain D2 with Robo receptors. If this is indeed the case, one would expect Slit D2 to display a similar heparin/HS-dependent activity as full-length Slit, even though it is lacking the C-terminal high affinity heparin-binding site of the full-length molecule. In a previous study, we used an endothelial cell migration assay to demonstrate biological activity of Slit D2 (5). A drawback of this assay is that endothelial cells express a divergent member of the Robo family, Robo4, whose role as a Slit receptor is controversial (19–21). In the absence of further studies, it is therefore difficult to attribute the effect of Slit on endothelial cells to a specific Robo receptor. Moreover, all studies into the HS requirement of Slit-Robo signaling so far have focused on (cells of) the nervous system (9–13, 22–24). To facilitate comparison with these studies, we therefore decided to use a chemotropic collapse assay on cultured *Xenopus* retinal growth cones.

In this assay, conditioned medium of cells expressing hSlit2 induces growth cone collapse in a Robo- and heparin/HS-dependent manner (8). We found that recombinant hSlit2 D2 protein (61.5 and 96.6% sequence identity to *Drosophila* and *Xenopus* Slit D2, respectively) applied at 40 nM (the optimal concentration determined in a dose-response experiment; data not shown) elicited a robust collapse response, comparable with that obtained with hSlit2 conditioned medium (Fig. 4, A–C and H). As expected from our previous analysis (5), other Slit domains were inactive (data not shown). Addition of heparin or HS had no effect on the collapse-inducing activity of hSlit2 D2 (Fig. 4, D, E, and H). In sharp contrast, enzymatic removal of HS from the neurites by heparinase treatment abolished the response to hSlit2 D2, demonstrating that Slit-Robo signaling does not occur in the absence of HS chains at the cell surface. Remarkably, addition of heparin to heparinase-digested growth cones fully restored their sensitivity to hSlit2 D2 (Fig. 4, G and H), indicating that, in this assay format, exogenous soluble heparin/HS can substitute for endogenous HS proteoglycans to support productive signaling. Taken together, the results demonstrate that the D2 domain of Slit contains not only the unique Robo-binding site but also a functionally important heparin/HS-binding site.

Location of the Heparin/HS-binding Site in Slit D2

We next wanted to determine which residues in Slit D2 contribute to heparin/HS binding. Because the role of HS in Slit-Robo signaling appears to be conserved between invertebrates and vertebrates (9–13, 22, 23), we looked for conserved basic residues that might be involved in HS binding. Because we wanted to test the mutants in the growth cone collapse assay, we chose hSlit2 D2 for mutagenesis. Using an alignment of invertebrate and vertebrate Slit sequences (Fig. 5A) and a molecular model of hSlit2 D2 (Fig. 5B), we selected a total of 12 basic residues for mutagenesis (Table 1). Mutants 1–4 target a basic patch in the N-terminal region of hSlit2 D2, and mutants 5–7 target a large concentration of basic charges in the C-terminal cap of the D2 domain (Fig. 5B). Both of these basic patches are adjacent to the Robo-binding site defined in our previous study (5).

All hSlit2 D2 mutants were purified to homogeneity from the conditioned medium of episomally transfected 293 cells (data not shown). Heparin affinity chromatography unexpectedly revealed that hSlit2 D2 has considerably higher affinity for heparin than its *Drosophila* orthologue (0.85 M NaCl required for elution, compared with 0.28 M for *Drosophila* Slit D2); the biological relevance of this difference (if any) remains to be established. Mutation of basic residues in the N-terminal half of hSlit2 D2 (mutants 1–4) had no effect on heparin binding, whereas mutation of basic residues in the C-terminal region (mutants 5–7 and the quadruple mutant 5 + 6) resulted in a substantial decrease of heparin affinity (Table 1). Crucially, when we examined the biological activity of two mutants that showed the most reduced heparin binding (mutants 7 and 5 + 6), we found that both mutants had lost the ability to trigger growth cone collapse (Table 1). These results demonstrate that the C-terminal cap region of Slit D2 harbors a functionally critical binding site for heparin/HS.

DISCUSSION

Several growth factors and cytokines require heparin/HS for productive signaling. The classic example is fibroblast growth factor (FGF), which requires HS as an obligatory co-receptor for signaling (25, 26). HS also binds to the FGF receptor (FGFR) (27), and specific HS sequences support signaling (16). Recent crystallographic studies have confirmed that a ternary complex is formed by these partners (28, 29). Although the structural details of the ternary signaling complex are still a matter of dispute, it is clear that an important role of heparin/HS is to stabilize the relatively weak binary interaction between FGF and FGFR.

In previous studies, HS was shown to be required for Slit-Robo signaling *in vitro* (9) and *in vivo* (10–13, 22–24), but the molecular mechanism(s) involved remained unclear. Our previous results have shown that Robo binds to a highly conserved site on the concave face of Slit D2 (5). In this study, we show that heparin/HS binding to a conserved basic patch adjacent to the Robo-binding site is critical for the biological activity of Slit D2. Furthermore, we provide direct biochemical evidence for a ternary complex consisting of Slit D2, Robo, and heparin. We conclude that heparin/HS is an integral and essential component of the Slit-Robo signaling complex.

Slit concentrations *in vivo* are likely to be much lower than the Slit D2 concentration required for growth cone collapse *in vitro*, and one function of the high affinity heparin-binding site in the C-terminal region of Slit may be to concentrate the Slit protein at the target cell surface or modulate its diffusion through extracellular matrix (12). This interpretation could explain why excess heparin/HS abolishes growth cone collapse triggered by full-length Slit (8, 9) but not by the isolated D2 domain (Fig. 4). We think that exogenous heparin/HS competes with cell surface HS for binding to the CT domain of the full-length protein, thereby preventing Slit recruitment to the growth cone surface. The D2

domain, in contrast, is present at 40 nM in our assay, and HS is no longer required for cell surface localization. Thus, we speculate that HS may play a dual role in Slit-Robo signaling, by acting both as a modulator of Slit distribution (12) and as an essential component of the signaling complex (this study). Slits are naturally processed by proteolytic cleavage within the EG5-EG6 linker (1). The functional relevance of Slit processing is currently not understood, but it is intriguing that cleavage results in the separation of the two heparin/HS-binding regions of Slit.

A number of previous studies *in vivo* have provided evidence to suggest that specific HS structures are involved in retinal axon guidance and Slit-Robo signaling (22–24, 30). Because Slit contains multiple heparin/HS-binding sites (Fig. 1), it is difficult to assess whether the observed effects are due to an effect on Slit distribution (HS binding to the CT domain) or signaling (HS binding to the D2 domain), or both. By applying recombinant D2 domain (mutants) and exogenous heparin derivatives to growth cones lacking cell surface HS, we should be able to define precisely the HS sequence(s) required for Robo activation. In this regard, it is interesting to compare the impact of Slit D2 mutations on heparin binding and biological activity. Even though we failed to disrupt heparin binding completely, we were able to abrogate all activity in the growth cone collapse assay. Evidently, the requirements for Slit D2 binding to cell surface HS are more stringent than for binding to heparin-Sepharose.

In conclusion, our results have revealed a specific role for heparin/HS in forming a ternary signaling complex with Slit D2 and Robo. At first glance, the parallels to the FGF-FGFR system are striking, but there are important differences that make it unlikely that the analogy extends to the mechanism of transmembrane signaling. First, Slits are large extracellular matrix proteins, whereas FGFs are small single-domain proteins. Second, Robos are cell adhesion molecules with no recognized catalytic activity in their cytosolic domains (7, 31), whereas FGFRs contain cytosolic tyrosine kinase domains. In the FGF-FGFR system, heparin/HS collaborates with FGF to promote receptor dimerization, which is required for FGFR autophosphorylation and downstream signaling (28, 29). In the Slit-Robo system, the oligomerization state of Robo and the mechanism of transmembrane signaling remain to be established. Conceivably, multiple Slit-Robo signaling complexes could be assembled upon a single HS chain, but Slit and HS could also disrupt an inactive Robo oligomer to initiate signaling.

REFERENCES

1. Brose K, Tessier-Lavigne M. *Curr. Opin. Neurobiol.* 2000; 10:95–102. [PubMed: 10679444]
2. Dickson BJ. *Science.* 2002; 298:1959–1964. [PubMed: 12471249]
3. Carmeliet P, Tessier-Lavigne M. *Nature.* 2005; 436:193–200. [PubMed: 16015319]
4. Hinck L. *Dev. Cell.* 2004; 7:783–793. [PubMed: 15572123]
5. Howitt JA, Clout NJ, Hohenester E. *EMBO J.* 2004; 23:4406–4412. [PubMed: 15496984]
6. Liu Z, Patel K, Schmidt H, Andrews W, Pini A, Sundaresan V. *Mol. Cell. Neurosci.* 2004; 26:232–240. [PubMed: 15207848]
7. Guan KL, Rao Y. *Nat. Rev. Neurosci.* 2003; 4:941–956. [PubMed: 14682358]
8. Piper M, Anderson R, Dwivedy A, Weinl C, van Horck F, Leung KM, Cogill E, Holt C. *Neuron.* 2006; 49:215–228. [PubMed: 16423696]
9. Hu H. *Nat. Neurosci.* 2001; 4:695–701. [PubMed: 11426225]
10. Inatani M, Irie F, Plump AS, Tessier-Lavigne M, Yamaguchi Y. *Science.* 2003; 302:1044–1046. [PubMed: 14605369]
11. Steigemann P, Molitor A, Fellert S, Jackle H, Vorbruggen G. *Curr. Biol.* 2004; 14:225–230. [PubMed: 14761655]

12. Johnson KG, Ghose A, Epstein E, Lincecum J, O'Connor MB, Van Vactor D. *Curr. Biol.* 2004; 14:499–504. [PubMed: 15043815]
13. Rhiner C, Gysi S, Frohli E, Hengartner MO, Hajnal A. *Development (Camb.)*. 2005; 132:4621–4633.
14. Couchman JR. *Nat. Rev. Mol. Cell Biol.* 2003; 4:926–937. [PubMed: 14685171]
15. Skidmore, MA.; Turnbull, JE. *Chemistry and Biology of Heparin and Heparan Sulfate*. Garg, H., editor. Elsevier Science Publishers B.V.; Amsterdam: 2005. p. 181-203.
16. Guimond SE, Turnbull JE. *Curr. Biol.* 1999; 9:1343–1346. [PubMed: 10574766]
17. Ronca F, Andersen JS, Paech V, Margolis RU. *J. Biol. Chem.* 2001; 276:29141–29147. [PubMed: 11375980]
18. Robinson CJ, Harmer NJ, Goodger SJ, Blundell TL, Gallagher JT. *J. Biol. Chem.* 2005; 280:42274–42282. [PubMed: 16219767]
19. Park KW, Morrison CM, Sorensen LK, Jones CA, Rao Y, Chien CB, Wu JY, Urness LD, Li DY. *Dev. Biol.* 2003; 261:251–267. [PubMed: 12941633]
20. Suchting S, Heal P, Tahtis K, Stewart LM, Bicknell R. *FASEB J.* 2005; 19:121–123. [PubMed: 15486058]
21. Kaur S, Castellone MD, Bedell VM, Konar M, Gutkind JS, Ramchandran R. *J. Biol. Chem.* 2006; 281:11347–11356. [PubMed: 16481322]
22. Lee JS, von der Hardt S, Rusch MA, Stringer SE, Stickney HL, Talbot WS, Geisler R, Nusslein-Volhard C, Selleck SB, Chien CB, Roehl H. *Neuron.* 2004; 44:947–960. [PubMed: 15603738]
23. Bulow HE, Hobert O. *Neuron.* 2004; 41:723–736. [PubMed: 15003172]
24. Pratt T, Conway CD, Tian NM, Price DJ, Mason JO. *J. Neurosci.* 2006; 26:6911–6923. [PubMed: 16807321]
25. Yayon A, Klagsbrun M, Esko JD, Leder P, Ornitz DM. *Cell.* 1991; 64:841–848. [PubMed: 1847668]
26. Rapraeger AC, Krufka A, Olwin BB. *Science.* 1991; 252:1705–1708. [PubMed: 1646484]
27. Kan M, Wang F, Xu J, Crabb JW, Hou J, McKeehan WL. *Science.* 1993; 259:1918–1921. [PubMed: 8456318]
28. Pellegrini L, Burke DF, von Delft F, Mulloy B, Blundell TL. *Nature.* 2000; 407:1029–1034. [PubMed: 11069186]
29. Schlessinger J, Plotnikov AN, Ibrahim OA, Eliseenkova AV, Yeh BK, Yayon A, Linhardt RJ, Mohammadi M. *Mol. Cell.* 2000; 6:743–750. [PubMed: 11030354]
30. Irie A, Yates EA, Turnbull JE, Holt CE. *Development (Camb.)*. 2002; 129:61–70.
31. Hivert B, Liu Z, Chuang CY, Doherty P, Sundaresan V. *Mol. Cell. Neurosci.* 2002; 21:534–545. [PubMed: 12504588]

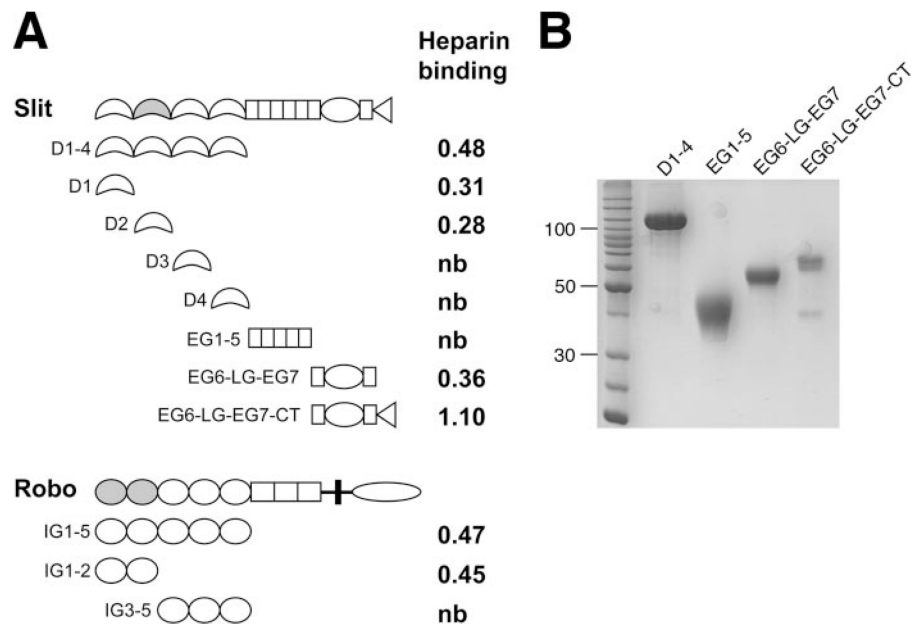


FIGURE 1. Heparin-binding sites in Slit and Robo

A, domain structure and heparin binding of *Drosophila* Slit and Robo constructs (*D1–4*, leucine-rich repeat domains; *EG*, epidermal growth factor-like domain; *LG*, laminin G-like domain; *CT*, C-terminal domain; *IG*, IG-like domain). Affinities for heparin are expressed as the molar NaCl concentration required for elution from a heparin HiTrap column (*nb*, no binding at physiological ionic strength). Full-length Slit and Robo are shown for reference; the domains responsible for their interaction (5, 6) are shaded *gray*, and the transmembrane segment of Robo is represented by a *vertical bar*. *B*, Coomassie Blue-stained SDS-polyacrylamide gel of selected Slit constructs. The molecular masses (in kDa) of selected markers are indicated on the *left*.

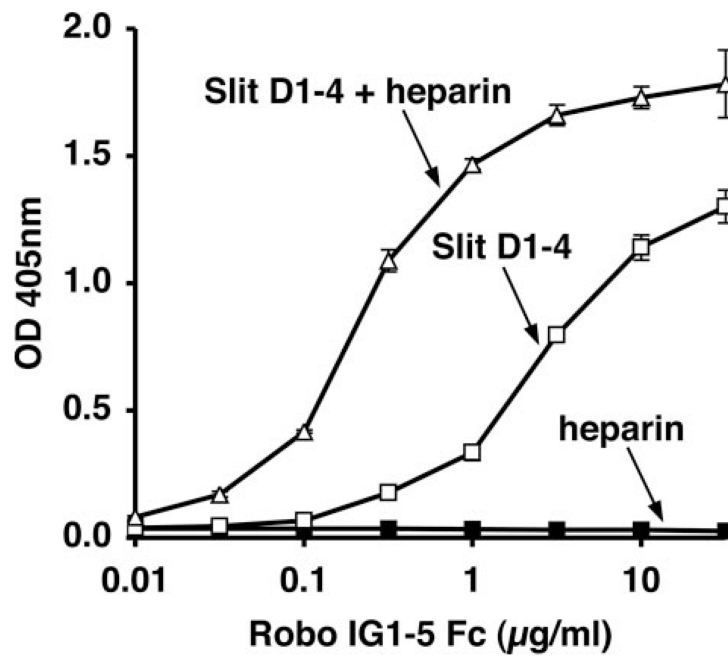


FIGURE 2. Heparin enhances the Slit-Robo interaction

Binding of soluble Robo IG1-5 Fc to immobilized Slit D1-4 in the absence and presence of 10 µg/ml heparin. Bound Robo IG1-5 Fc was detected by alkaline phosphatase-conjugated anti-Fc antibody. 1 µg/ml Robo D1-5 Fc corresponds to 25 nM Robo monomer. Values are presented as mean ± S.E. ($n = 3$).

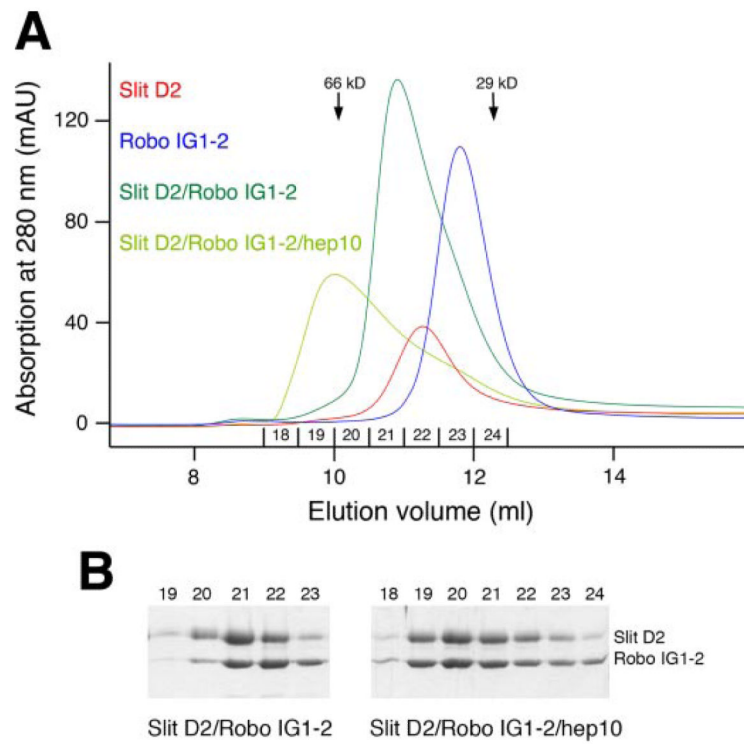


FIGURE 3. Gel filtration analysis of a minimal ternary Slit-Robo-heparin complex

A, gel filtration chromatograms of isolated *Drosophila* Slit D2 and Robo IG1–2, a 1:1 mixture of the two proteins, and a 1:1:1 mixture of the two proteins with a heparin-derived decasaccharide (*hep10*). The elution volumes of two globular molecular mass standards are indicated by *vertical arrows* (albumin, 66 kDa; carbonic anhydrase, 29 kDa). The void volume of the column is 8.0 ml. The fractions collected for SDS-PAGE analysis are indicated. *B*, Coomassie Blue-stained SDS-PAGE gel of the peak fractions indicated in *A*. The fraction numbers are shown at the *top*.

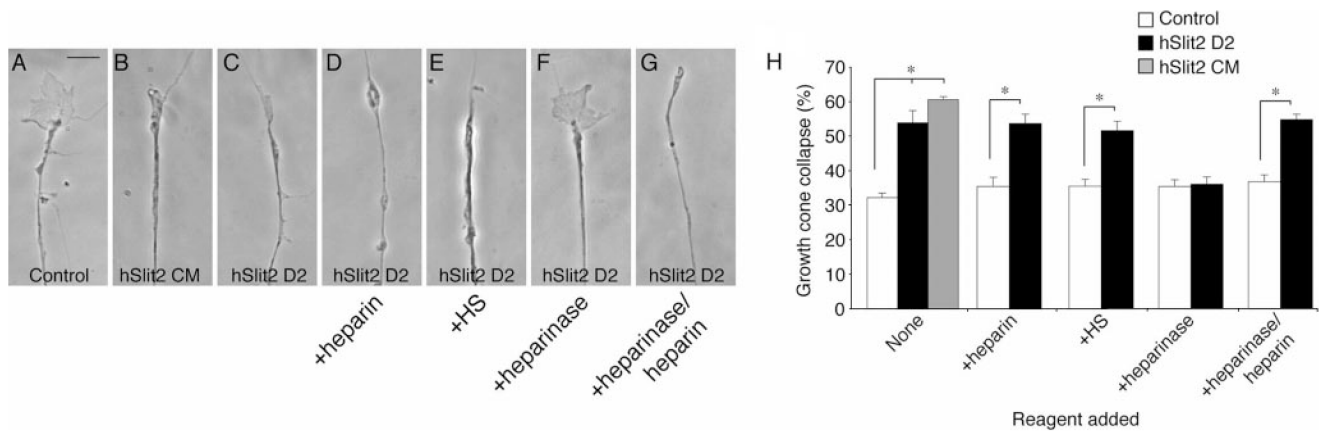


FIGURE 4. Heparin/HS-dependent collapse of *Xenopus* retinal growth cones by hSlit2 D2
 Growth cones were treated with TBS buffer control (A), conditioned medium of hSlit2-expressing cells (B), and 40 nM of purified hSlit2 D2 (D--G). Heparin (D and G) or HS (E) was added at a concentration of 100 $\mu\text{g/ml}$, and in some experiments (F and G) growth cones were pretreated with heparinase 1 (2.5 units/ml). H, quantification of the collapse data shown in A–G. Values are presented as percentage of growth cone collapse \pm S.E. *, $p < 0.03$, two-tailed Mann-Whitney *U* test. Scale bar, 5 μm .

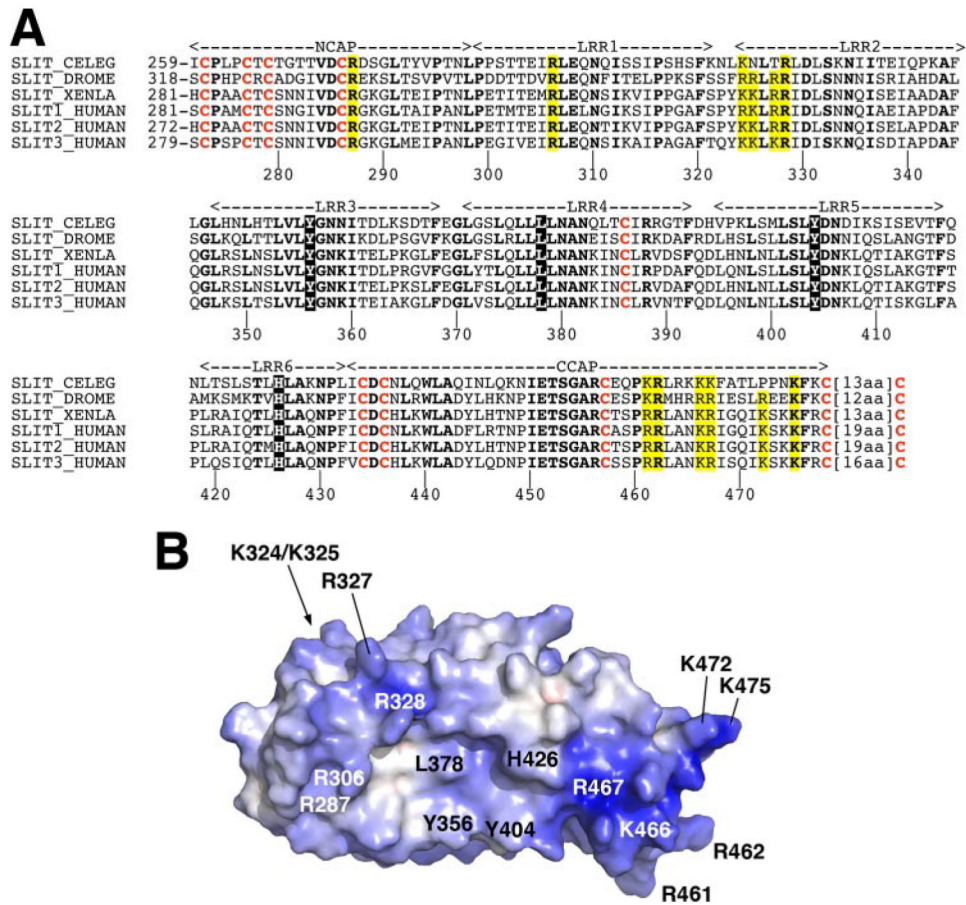


FIGURE 5. Location of conserved basic residues in hSlit2 D2

A, alignment of D2 domain sequences from *Caenorhabditis elegans*, *Drosophila melanogaster*, and *Xenopus laevis* Slit and human Slit1–3. Conserved residues are in *boldface*; cysteines are *red*; residues involved in Robo binding (5) are *shaded black*, and basic residues mutated in this study (see Table 1) are *shaded yellow*. The domain structure is indicated above the alignment (NCAP and CCAP, cap domains; LRR1–6, leucine-rich repeats 1–6). The hSlit2 sequence numbering is given below the alignment. *B*, electrostatic surface representation of a molecular model of hSlit2 D2. Positive and negative potential is indicated by *blue* and *red* coloring, respectively. The view direction is onto the concave face of the D2 domain, with the N- and C-terminal caps at the *left* and *right*, respectively. The location of residues involved in Robo binding (Tyr³⁵⁶, Leu³⁷⁸, Tyr⁴⁰⁴, and His⁴²⁶) and of basic residues mutated in this study are labeled.

TABLE 1
Heparin binding and growth cone collapse activity of hSlit2 D2 mutants

Heparin binding is expressed as the molar NaCl concentration required for elution from a heparin HiTrap column. The growth cone collapse assay was performed and quantified as in Fig. 4 (ND indicates not determined).

	Mutations	Heparin binding	Percent growth cone collapse \pm S.E.
TBS			26.7 \pm 1.5
Wild type		0.85	60.2 \pm 3.1
Mutant 1	R287A	0.84	ND
Mutant 2	R306A	0.86	ND
Mutant 3	K324A/K325A	0.83	ND
Mutant 4	R327A/R328A	0.85	ND
Mutant 5	R461A/R462A	0.64	ND
Mutant 6	K466A/R467A	0.69	ND
Mutant 7	K472A/K475A	0.58	26.8 \pm 5.4
Mutant 5 + 6	R461A/R462A/K466A/R467A	0.48	35.0 \pm 3.5